



Research article

Ameliorative effect of cheqianzi decoction on hyperuricemia and kidney injury and underlying mechanism in rats

Jing Meng¹, Jingzhuo Tian¹, Yong Zhao, Chunying Li, Yan Yi, Yushi Zhang, Jiayin Han, Lianmei Wang, Chen Pan, Suyan Liu, Chenyue Liu, Fang Wang, Xuan Tang, Dunfang Wang, Shasha Qin, Aihua Liang^{*}

Institute of Chinese Materia Medica, China Academy of Chinese Medical Sciences, Beijing, China



ARTICLE INFO

Keywords:

Cheqianzi decoction (CQD)
Hyperuricemia (HUA)
Kidney injury
ABCG2
NLRP3

ABSTRACT

Cheqianzi Decoction (CQD) is a Traditional Chinese Medicine (TCM) formula comprising four herbs and is recorded in the Ancient Materia Medica “Shengji Zonglu”. Individually, these four herbs have been shown to reduce uric acid (UA) levels, to treat hyperuricemia (HUA), and alleviate kidney damage. However, the therapeutic efficacy of the CQD and related mechanism are not yet clear.

In this study, high performance liquid chromatography (HPLC) analysis confirmed that the contents of the chemical components of the four herbal medicines were in accordance with the provisions of the Chinese Pharmacopoeia. A total of 99 potential targets were identified in the network pharmacology analysis of CQD, indicating its involvement in the regulation of inflammatory and apoptotic signaling pathways, and potential value for treating HUA and alleviating kidney injury. In vivo pharmacodynamic studies showed that compared with the Model group, significantly decreased levels of serum uric acid (SUA), serum creatinine (SCr), blood urea nitrogen (BUN) (all $P < 0.05$), and inflammatory factors ($P < 0.01$) were detected in the CQD group. Quantitative real-time PCR and Western blot analyses showed that compared with the Model group, adenosine triphosphate (ATP)-binding cassette efflux transporter G2 (ABCG2) expression in the CQD group was significantly upregulated ($P < 0.01$) at both the mRNA and protein levels, while mRNA expression of Caspase3 and NOD-like receptor family member 3 (NLRP3) ($P < 0.05$) and protein expression of NLRP3 ($P < 0.01$) were significantly downregulated.

In conclusion, CQD promotes UA excretion by activating ABCG2, and induces inflammasome NLRP3-mediated reduction in inflammatory and apoptotic factors to achieve renal protection. Thus, our findings indicate the therapeutic potential of CQD in HUA with kidney injury.

1. Introduction

Hyperuricemia (HUA) is a metabolic syndrome characterized by a high level of UA in the blood due to abnormal purine metabolism. HUA is a common disease that has increased in prevalence with improvements in living standards, also showing an increase in

^{*} Corresponding author. Institute of Chinese Materia Medica, China Academy of Chinese Medical Sciences, No. 16 Nanxiaojie, Dongzhimen Nei Ave, Beijing, 100700, China.

E-mail address: ahliang@icmm.ac.cn (A. Liang).

¹ Authorship note: Joint first authors.

a younger population. According to nationally representative cross-sectional surveys, the prevalence of HUA among Chinese adults was 11.1% in 2015–16 and increased to 14.0% in 2018–19 [1]. In addition to being closely related to gout, HUA is also considered to be an independent risk factor for many diseases, including chronic kidney diseases, cardiovascular diseases, hypertension, and other metabolic syndrome disorders such as diabetes [2–5]. Furthermore, the degree of kidney injury in patients with HUA increases gradually with the SUA level [6]. At present, the drugs commonly used to treat HUA include xanthine oxidase inhibitor (allopurinol and Febuxostat) and UA reabsorption inhibitors (benzbromarone and probenecid) [7,8]. Although these drugs show good effects in reducing SUA, they do not significantly improve kidney injury associated with HUA [9], and can induce adverse reactions such as hepatotoxicity, increased cardiovascular risk and severe drug eruption, and even death [10–12]. Therefore, research is now focused on the development of therapeutic approaches that effectively control UA levels in sera and offer renal protection.

Traditional Chinese Medicines (TCMs) with the functions of heat-clearing, detoxification, diuresis and dehumidification are likely to produce good curative effects on the pathogenesis of HUA [13]. The CQD, which is composed of extracts of *Plantaginis Semen* (cheqianzi), *Achyranthis Bidentatae Radix* (niuxi), *Typhae Pollen* (puhuang) and *Mori Cortex* (sangbaipi), was recorded in volume 98 of “Shengji Zonglu” in the Song Dynasty, and has marked therapeutic effects on heat stranguria, stagnation and astringency. Most modern research associates HUA with heat stranguria [14]. Drugs that induce diuresis are widely used to treat HUA, indicating that the diuretic effects of CQD may be beneficial for the treatment of this condition. According to the records of the Chinese Pharmacopoeia, these four herbal medicines all have the effects of promoting urination and relieving inflammation. Cheqianzi has been reported to have potential therapeutic effects on HUA [15]. A lipidomic study confirmed that cheqianzi produces significant anti-HUA, anti-inflammatory and renoprotective effects by regulating lipid metabolism [16]. Acteoside, the active ingredient in cheqianzi, has also been reported to reduce SUA levels by inhibiting UA production and preventing its reabsorption [17]. Niuxi has renoprotective effects thought to be related to its capacity to inhibit apoptosis and oxidation by regulating inflammatory responses and through estrogen-like effects [18]. Sangbaipi reduces the levels of inflammatory factors, inhibits the UA reabsorption, while promoting its excretion, thereby reducing UA levels and protecting the kidneys [19]. The combination of ancient records and modern pharmacological studies of herbs suggests the therapeutic potential of CQD in HUA.

The discipline of network pharmacology aims to explore the multilevel interactions of drugs, diseases and targets as a whole [20] to provide a basis for understanding the mechanism of action and the development of multi-target drugs [21]. In this study, we explored the compatibility of these herbs in CQD for their therapeutic effects on HUA and alleviating kidney injury as well as the underlying mechanisms based on network pharmacology analysis to provide a theoretical basis for the development of new treatments for HUA using CQD.

2. Materials and methods

2.1. Materials and reagents

The following materials and reagents were used in this study: geniposidic acid, verbascoside, typhaneoside, isorhamnetin-3-O-neohesperidoside, β -ecdysterone and chlorogenic acid chemical composition standard (all purity >95%) were obtained from Yuan-ye Biotechnology Co., Ltd. (Shanghai, China). Ethambutol (Ethb) (Jinhua, Chengdu, China). Adenine (AD) (Sigma-Aldrich, USA). Allopurinol (Allo) (Shimao Tianjie, Yancheng, China). UA, SCr, BUN test kits (Dibao Medical Supplies, Guangzhou, China). Urate staining solution (Gomori), hematoxylin eosin (HE) (Solarbio, Beijing, China). Interleukin-6 (IL-6), tumor necrosis factor- α (TNF- α), interleukin-1 β (IL-1 β), interleukin-18 (IL-18) Enzyme-linked immunosorbent assay (ELISA) kits (R&D Systems, USA). The following primary antibodies were used for immunoblotting: anti-ABC2 (Cat No. 4477s, 1:1,000, Cell Signaling Technology, USA), anti-NLRP3 (Cat No. ab263899, 1:1,000, Abcam, UK) and anti-GAPDH (Cat No. sc-365062, 1:1,500, Santa Cruz Biotechnology, USA).

2.2. Preparation of CQD

According to the Shengji Zonglu medical encyclopedia compiled by the government in the Northern Song Dynasty, CQD is a mixture of 1 liang (两) Cheqianzi, 1 liang niuxi, 3 liang sangbaipi, and 1 liang puhuang. CQD is administered at 2 qianbi (钱匕) per dose, and the number of doses depends on the patient's needs. According to previously published studies of the Song Dynasty prescription doses [22], 1 liang is approximately equal to 40 g. After conversion, the modern clinical dosage of CQD does not correspond with the dosage according to ancient prescription records. Due to this discrepancy and because the number of doses is unlimited in the ancient prescription records, the proportion of the original prescription was used as the basis for determining the dosage of CQD used in this study. According to the current Chinese Pharmacopoeia, the maximum clinical dosage of sangbaipi in the prescription is 12 g, and proportionally, maximum clinical dosage of the other herbs is 4 g. This dose was set to best match the usual clinical dose. Due to the absence of reports on CQD research, this experimental dose formed the basis of subsequent drug development. The herbs were purchased from Beijing Tongrentang Co., Ltd. and identified by Huasheng Peng, from the Chinese Medicine Resource Center of China Academy of Chinese Medical Sciences (CACMS) with the following results: Cheqianzi from *Plantago asiatica* L. and *Plantago depressa* Willd. dry mature seeds; niuxi from the dry roots of *Achyranthes bidentata* BL; sangbaipi from the dry root bark of *Morus alba* L.; puhuang from the dried pollen of *Typha angustifolia* L., *Typha orientalis* Presl or the same genus in Typhaceae. All plants were verified and approved by the Medicinal Plant Names Services (<http://mpns.kew.org>) on September 20, 2022. The herbs were soaked at a ratio of 1:1:3:1 (w/w/w/w) in 15-fold volumes of distilled water (v/w) for 30 min, and the seeds of cheqianzi and puhuang were wrap-decocted. After the first decoction, the same volume of distilled water was added and the process was repeated. After filtration, the solution was evaporated under reduced pressure to yield a suspension with a final concentration of 0.432 g/ml and stored at 4 °C

for further use.

2.3. HPLC analysis of CQD

To identify the components of CQD, we performed HPLC analysis using a Waters 2998. Infinity chromatographic system fitted with a C18 chromatographic column (250 × 4.6 mm, 5 μm, Agilent, USA), a column oven, a binary pump, a diode array detector, and an autosampler (Waters, USA). After washing, the column was activated for injection analysis. Throughout the whole chromatographic analysis process, the column injector was maintained at 30 °C. The mobile phase consisted of methanol (A; Thermo Fisher Scientific, USA) and 0.05% acetic acid aqueous solution (B; Beijing, China). A gradient elution was performed with 5% A from 0 to 1 min, 5%–60% A from 1 to 40 min, 60%–5% A from 40 to 50 min, and 5% A from 50 to 60 min. After full wavelength scanning, the detection wavelength was set at 260 nm and each compound was identified according to the pure standard absorbance spectra and retention time.

2.4. Systemic pharmacological analysis of CQD

2.4.1. Collection and screening of bioactive compounds in CQD

The active ingredients of CQD were screened before the China National Knowledge Infrastructure (CNKI) website was searched to identify relevant literature on the analysis of the chemical composition of TCMs. The corresponding chemical composition information was then screened using the CAS Ichemistry (<http://www.ichemistry.cn/>), Chemical Book (<https://www.chemicalbook.com/>), ChemSpider (<http://www.chemspider.com/>) and other databases to obtain the corresponding English names and CAS numbers of chemical components, to eliminate duplicates, and determine the main active ingredients of each Chinese medicine.

2.4.2. Recognizing CQD compounds and predicting functional targets

The functional targets were predicted based on the main active ingredients using the BATMAN-TCM analysis platform (<http://bionet.ncpsb.org.cn/batman-tcm/>). This online bioinformatics analysis tool designed for the study of the molecular mechanisms underlying the effects of TCM [23] can be used to predict the potential targets of herbs and their component extracts. The scores of the interaction between all candidate targets and drug components are obtained by the target prediction algorithm, with the potential drug target identified as that with the highest score using an artificially defined “score cutoff point” [24]. In this study, the “score cutoff” was set at to 5.785 with an adjusted *P*-value of 0.05 to maximize the coverage of potential targets.

2.4.3. Identification of potential HUA-associated targets

Potential HUA-associated targets were identified by using the keyword “hyperuricemia” to search the following databases: OMIM (<https://www.omim.org/>), GeneCards (<https://www.genecards.org/>), CTD (<http://ctdbase.org/>), DisGeNET (<https://www.disgenet.org/>), HPO (<https://hpo.jax.org/app/>), DrugBank (<https://www.drugbank.ca/>), and NCBI-Gene (<https://www.ncbi.nlm.nih.gov/gene/>). In addition, referring to the disease-related diagnosis and treatment guidelines and literature, we searched for clinical drugs used to treat HUA, and supplementary information related to their corresponding targets. After removing the duplicated genes, the seven target subsets obtained in these steps were cross-referenced, and the remaining were identified as potential targets for the treatment of HUA.

2.4.4. Protein-protein interaction (PPI) network construction

Based on a Venn diagram of drug targets and HUA targets constructed using the Venny 2.1.0 software online platform (<https://bioinfogp.cnb.csic.es/tools/venny/index.html>), the intersection was defined as the potential targets of CQD in the treatment of HUA. For PPI analysis, the targets were then introduced into STRING (<https://string-db.org/>), an online PPI analysis database used to analyze each protein-protein interaction based on scoring evidence from multiple sources [25]. After importing the target information, the species was limited to “*Homo sapiens*” and the minimum required interaction score was set at a confidence value of 0.500 to obtain PPI data, which was saved as a tsv. format file for further exploration.

2.4.5. Screening and evaluation of key targets and active compounds

The data obtained in the STRING database analysis were imported into Cytoscape 3.8.2 (<https://cytoscape.org/>), which is an open-source software that provides many bioinformatics analysis tools for network analysis. The PPI network was constructed before network analysis was performed to obtain the core targets using the median of degree, closeness, and between-ness as the limiting conditions. Finally, the core targets that met these criteria were sequentially mapped to the CQD components using the “VLOOKUP” function to build a correlation network of “CQD-compounds-core targets-diseases”.

2.4.6. Gene ontology (GO) and Kyoto encyclopedia of genes and genomes (KEGG) pathway enrichment analyses

To elucidate the biological processes of the core targets in different clusters and their roles in signaling transduction, we performed GO and KEGG pathway enrichment analysis using Metascape (<https://metascape.org>). Next, custom analysis was performed by entering a list of target gene names with the minimum overlap set to 3, with a *P*-value <0.01, and a minimum enrichment of 1.5. Finally, the top 20 entries were entered into a bubble chart for visualization using the online bioinformatics website (<http://www.bioinformatics.com.cn/>).

2.5. Animal pharmacodynamics validation

2.5.1. Establishment of the rat model of HUA and treatment

Our network pharmacology analysis indicated the therapeutic potential of CQD for HUA and possible anti-inflammatory effects. Therefore, we validated the pharmacodynamics of these predictions in a previously established rat model of HUA with mild kidney injury [26]. Twenty-four male specific pathogen-free grade Sprague-Dawley (weight 180 ± 10 g) were purchased from Beijing Vital River Laboratory Animal Technology (certificate number SCXK (Beijing) 2016-0006). Animals were housed in laboratory facilities maintained at 20–26 °C and a relative humidity of 40%–70%, with air changes at least 15 times per hour and a standard 12-h light/dark cycle. Six rats were housed in one cage, and were given free access to a quantitative fixed-formula granular feed and filtered tap water. All procedures used in the animal experiments adhered to a protocol that had been approved by the Institutional Animal Care and Use Committee of the Institute of Chinese Materia Medica, CACMS (Ethics number: 2020B127). 24 rats were fed freely for one week without any intervention, and then randomly divided into four groups ($n = 6$ rats per group) as follows: Control, Model, CQD, and Allo (positive control) groups. From the first day of the experiment, the two treatment groups and Model group were intragastrically administered a mixed modeling drug containing $100 \text{ mg kg}^{-1}\cdot\text{d}$ AD solution and $250 \text{ mg kg}^{-1}\cdot\text{d}$ Ethb solution, while the Control group received an equal amount of 1% CMC-NA via the same route. The treatment groups received CQD or $20 \text{ mg kg}^{-1}\cdot\text{d}$ Allo solution while the model was established, and the rats in Control and Model groups received the same amount of saline. The dose of CQD was converted from the human clinical equivalent dose. The modeling and treatment process was continued for 7 days.

2.5.2. Collection of blood and urine

After 3 days of intervention, urine and orbital blood samples were collected manually from all rats. After 7 days of intervention, each rat was placed in a metabolic cage for 10 h, and the urine was collected and weighed. After euthanization by intraperitoneal injection of 20% ethyl carbamate solution, blood was collected from the abdominal aorta and the kidneys were removed, photographed and weighed. The kidney index (%) was calculated as kidney weight (g)/fasting body weight (g) $\times 100\%$.

2.5.3. Detection of biochemical index and histopathological evaluation

Blood samples collected after 3 days and 7 days of intervention were centrifuged at 3500 rpm for 15 min at 4 °C. Serum levels of SUA, Scr and BUN were detected using an automatic biochemical analyzer (Toshiba, Japan). Urine was centrifuged under the same conditions and UUA content was determined. The left kidney was cut along the longitudinal axis. Half of the kidney was immersed in 10% neutral formalin, and then routinely dehydrated, embedded in paraffin, sectioned and stained with HE to evaluate the morphological changes. The other half of the kidney was soaked in absolute ethanol and Gomori staining was performed to evaluate urate deposition.

2.6. Detection of inflammatory factors

Kidney tissue stored at -80 °C was thawed and a portion (approximately 100 mg) of the tissue was cut away with scissors. After adding 10 times the volume of pre-cooled PBS, the tissue was homogenized and placed at -20 °C overnight and then thawed; this freeze-thaw process was repeated twice. The resulting homogenate was centrifuged at 5,000 rpm for 15 min at 4 °C and the supernatant was collected immediately for measurement of the inflammatory factors IL-6, TNF- α , IL-1 β and IL-18 by ELISA.

2.7. RT-PCR

Total RNA was extracted from kidney tissue using TRIzol reagent according to the manufacturer's instructions. After filtration and washing, the RNA was reverse transcribed into cDNA, for use as a template in the RT-PCR analysis. Primers were designed based on sequences identified in PubMed searches, and synthesized by Sangon Biotech (Shanghai); details of the primers are shown in [Supplementary Table 1](#). Two-step detection was performed with GAPDH as the internal reference, and relative gene expression was calculated using the $2^{-\Delta\Delta C_t}$ method.

2.8. Western blot analysis

Kidney tissue stored at -80 °C was thawed and a portion (approximately 60 mg) was placed in RIPA lysis buffer containing and PMSF inhibitor for homogenization on ice for 30 min. After centrifugation at 14,000 rpm for 5 min at 4 °C, the protein concentration of the supernatant was determined using a BCA assay (Beyotime, Shanghai, China). After adding loading buffer and denaturation at 100 °C for 5 min, approximately 50 μg of total proteins per sample were separated by SDS-PAGE and transferred to a PVDF membrane. After blocking with 5% dried skimmed milk, the membranes were washed with 0.2% Tween-20 PBS and incubated overnight at 4 °C with primary detection antibodies (anti-ABCG2, anti-NLRP3 and anti-GAPDH). The membranes were then incubated with a horseradish peroxidase-conjugated secondary antibody for 2 h at room temperature. Bands were visualized by enhanced chemiluminescence and analyzed using the Protein Simple Imaging system. The integrated optical density of each band was analyzed using ImageJ.

2.9. Statistical analysis

All statistical analyses were performed using SPSS 20.0 software. Data were presented as mean \pm standard deviation (SD). One-way

ANOVA was used for comparison of groups. For normally distributed data, the LSD method was used for analysis; otherwise the Tamhane's T2 method was used. Graphs were generated using Prism 8.0 software (GraphPad software, USA), and $P < 0.05$ was considered to indicate statistical significance.

3. Results

3.1. HPLC analysis of CQD

According to the provisions of the Chinese Pharmacopoeia, the following six chemical components were detected as landmark components of CQD: (A) geniposidic acid, (B) chlorogenic acid, (C) verbascoside, (D) typhaneoside, (E) isorhamnetin-3-O-neohesperidoside, (F) β -ecdysterone, among which cheqianzi, niuxi, and puhuang have the corresponding components determined in the Pharmacopoeia, while sangbaipi is not mentioned. Through reviewing the literature [27,28], we found that chlorogenic acid can be used as a standard to verify the quality of sangbaipi. The HPLC chromatograms (Fig. 1a–f) indicated that the main chemical components of each herb complied with the Pharmacopoeia regulations, and were suitable for subsequent experiments.

3.2. Network construction and analysis

3.2.1. CQD-active compound network analysis

After searching the relevant literature, we found that the TCMs cheqianzi, niuxi, puhuang and sangbaipi contained 111, 151, 100 and 218 compounds, respectively. The four TCM contained 7, 14, 18 and 10 superposed components, respectively, which are 23 components. The four TCMs had 104, 137, 82, and 208 unique active ingredients, respectively (Supplemental Figure S1). These results suggested that different TCMs with the same pharmacological effects may have the same components. Different herbs contain a variety of effective components, which is an important material basis for the multi-target effects of TCMs.

3.2.2. Identification of CQD and HUA-related targets

By screening the target scores, we identified 16,086, 31,990, 25,810, and 33,928, corresponding targets of cheqianzi, niuxi, puhuang, and sangbaipi, respectively. After standardization, a combined total of 4101 targets of the four TCMs were identified, demonstrating that many compounds share the same targets. Subsequently, 16,705 targets related to "HUA" were retrieved from multiple databases. Targets shared by at least two databases were screened, and after removal of duplicates, 740 targets were retained as HUA-related targets.

3.2.3. Protein-PPI network of CQD therapeutic targets for HUA

The intersection of CQD and HUA targets contained 392 common drug-disease targets (Fig. 2a). These 392 targets were screened using STRING to obtain the corresponding PPI network (Fig. 2b). Each node represents all proteins produced by a single protein-coding gene locus, and the edges represent protein-protein associations. The thickness of the network edge indicates the strength of data support. According to the confidence level, there were 390 network nodes and 4528 edges. The network was found to contain the corresponding UA-related transporters, while the dense central region contained mostly inflammation-related targets, suggesting that

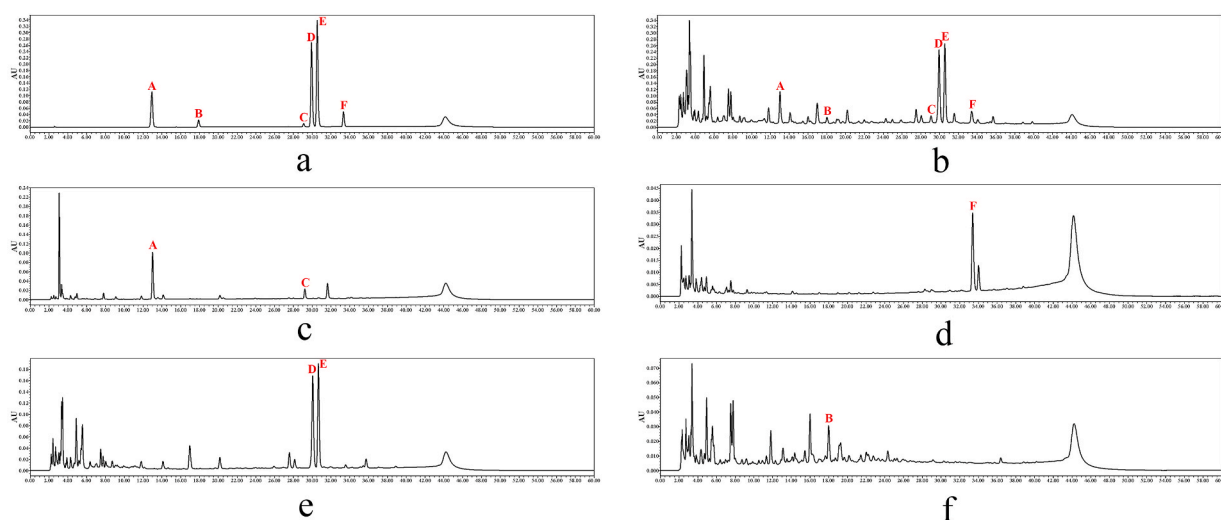


Fig. 1. HPLC chromatograms. (a) HPLC chromatogram of six chemical standards. A–F represent the following chemical standards: geniposidic acid, chlorogenic acid, verbascoside, typhaneoside, isorhamnetin-3-O-neohesperidoside and β -ecdysterone. (b) HPLC chromatogram of CQD. (c) HPLC chromatogram of Cheqianzi. (d) HPLC chromatogram of Niuxi. (e) HPLC chromatogram of Puhuang and (f) HPLC chromatogram of Sangbaipi.

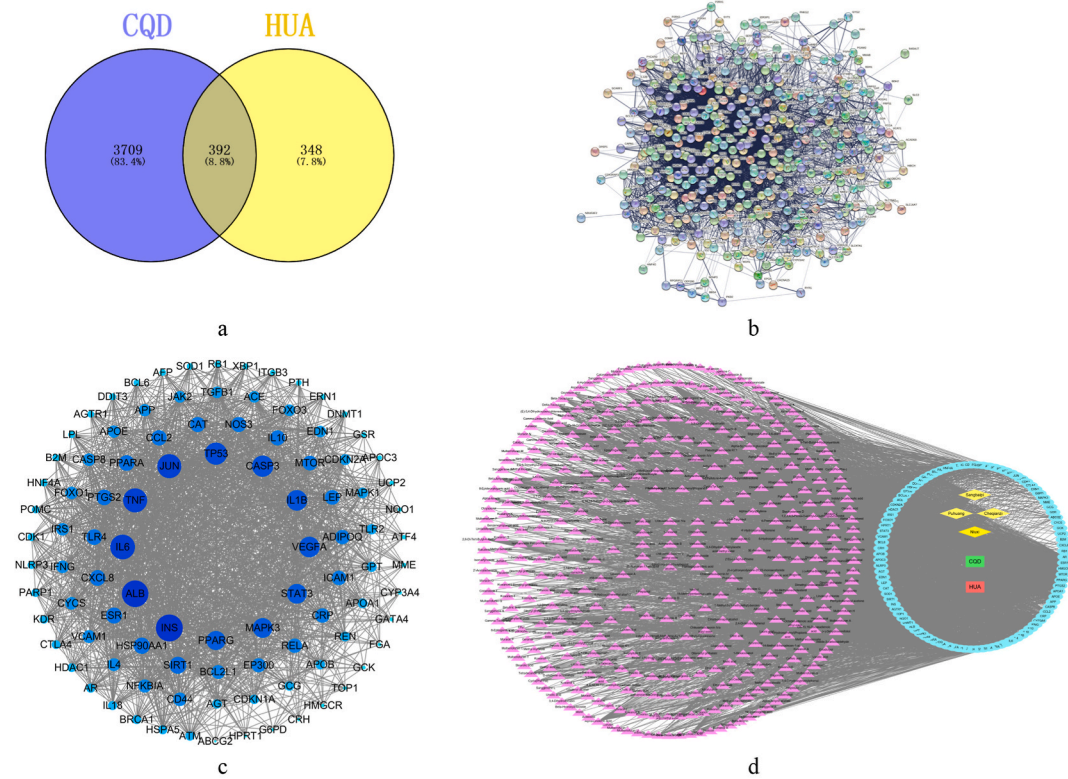


Fig. 2. Network pharmacology analysis results. (a) Venn diagram showing the targets of CQD (blue circle) and HUA (yellow circle), with the common core targets shown in the overlapping region. (b) PPI network of CQD targets against HUA. (c) Key targets of CQD against HUA. (d) CQD compound target-HUA network. The green and red rectangles represent the nodes of CQD and HUA. The yellow diamonds represent the nodes of the four herbs. The blue circle represents the core targets nodes. The purple triangle represents the nodes of the CQD compounds corresponding to core targets. (For interpretation of the references to color in this figure legend, the reader is referred to the Web version of this article.)

CQD reduces UA levels and exerts nephroprotective effects through an anti-inflammatory mechanism.

3.2.4. The CQD-compound-target-HUA network

Screening of the 390 targets identified in STRING using Cytoscape yielded 99 corresponding core targets (Fig. 2c). Most of the targets with higher scores were related to inflammation, such as IL-6, TNF- α , IL-1 β , IL-18, and NLRP3. A study showed a strong correlation between NLRP3 activation and high expression of inflammatory factors, such as IL-6, TNF- α , IL-1 β , and IL-18 [29].

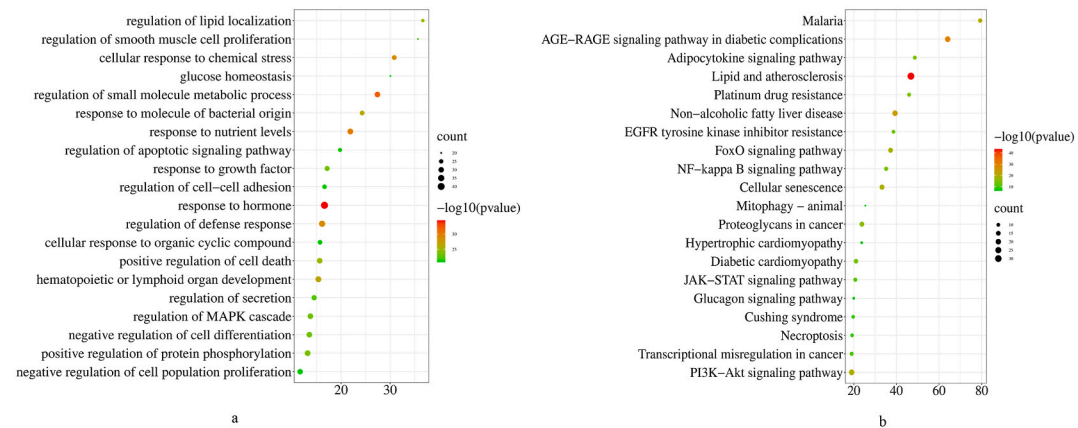


Fig. 3. GO and KEGG analysis results. (a) GO analysis of candidate targets. (b) KEGG pathway enrichment analysis result. The size of each node indicates enriched counts, the abscissa represents the enriched gene ratio, and the color indicates the enriched adjusted *P*-value. (For interpretation of the references to color in this figure legend, the reader is referred to the Web version of this article.)

Combined with other reports, this study indicated that the increase in levels of inflammatory factors and activation of the NLRP3 inflammasome caused by soluble UA is closely related to some kidney diseases [30,31], suggesting that the anti-inflammatory effect of CQD contributes to its nephroprotective effect. In addition, CQD-related core targets also include the ABCG2 transporter [32], dysfunction of which is a common mechanism for inducing UA production, leading to decreased extrarenal urate excretion and increasing the prevalence of HUA [33]. These findings suggested that CQD promotes UA excretion by upregulating the expression of ABCG2. A “CQD-compound-target-disease network diagram” representing the interactions between CQD and herbs, herbs and compounds, compounds and targets, and targets and diseases is shown in Fig. 2d.

3.2.5. GO and KEGG pathway enrichment analyses

To explore the molecular mechanism underlying the effects of CQD on HUA, we performed GO and KEGG pathway enrichment analyses of the 99 candidate targets. In total, 1727 different entries were found in the GO analysis, most of which were related to categories including response to hormone, regulation of defense response, regulation of small molecule metabolic process, and regulation of apoptosis signaling pathway. Statistical analysis suggested that response to hormone and regulation of small molecule metabolic process were closely related to the effects of CQD on HUA (Fig. 3a). Furthermore, 177 items were found in the KEGG pathway enrichment analysis, of which the main pathways included lipid and atherosclerosis, AGE-RAGE signaling pathway in diabetic complications, and the NF- κ B signaling pathway (Fig. 3b); the lipid and atherosclerosis pathway was identified as the most important and therefore, selected for further analysis.

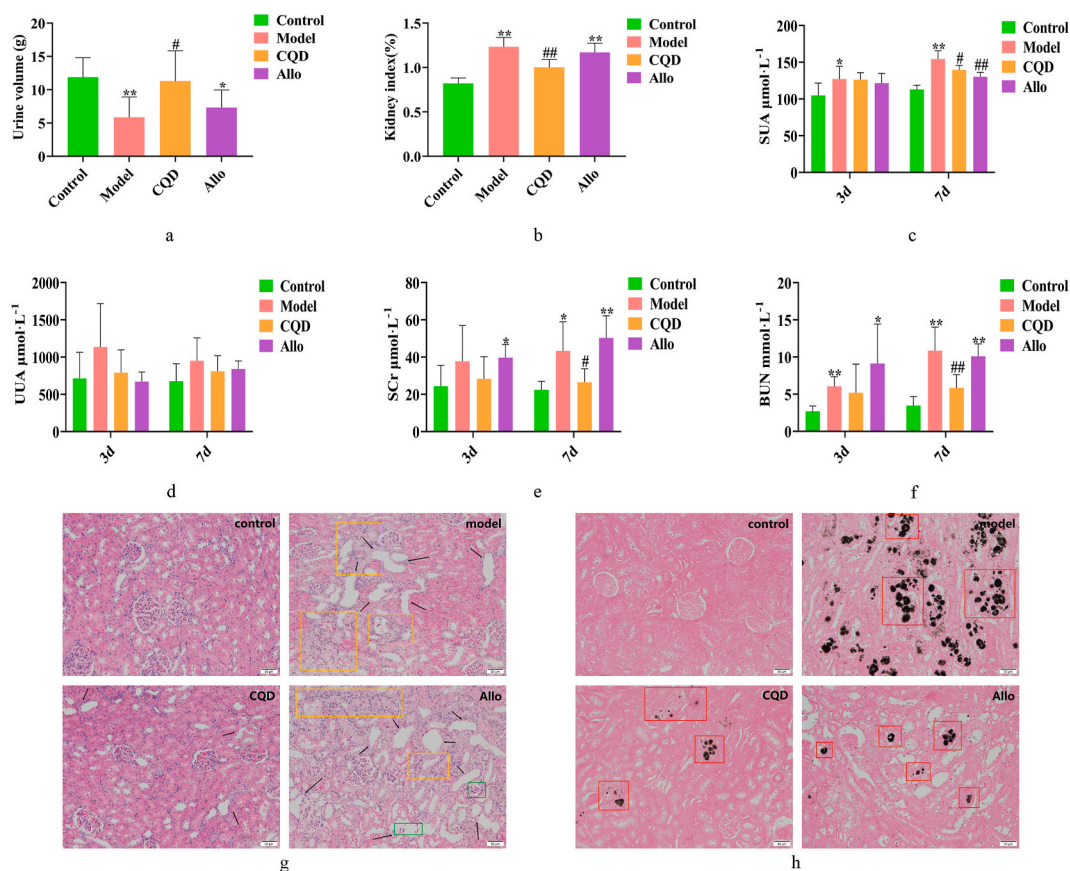


Fig. 4. Biochemical and pathological effects of CQD in rats. (a) Effect of CQD on urine volume. (b) Effect of CQD on kidney index. (c) Effect of CQD on SUA concentration. (d) Effect of CQD on UUA concentration. (e) Effect of CQD on SCr concentration. (f) Effect of CQD on BUN concentration. Data represent the mean \pm standard deviation (SD). * $P < 0.05$ and ** $P < 0.01$ vs Control group. # $P < 0.05$ and ## $P < 0.01$ vs. Model group. (g) Effect of CQD on renal histopathology. The black arrow indicates dilated renal tubules. The yellow and green rectangles indicate inflammatory cells and sloughed cells, respectively (HE staining). (h) Effect of CQD on urate deposition in renal tissues. The red rectangle indicates the urate crystals in rat kidneys (Gomori staining). Scale bar: 50 μ m. (For interpretation of the references to color in this figure legend, the reader is referred to the Web version of this article.)

3.3. CQD reduces UA and alleviates kidney injury in rats

3.3.1. Effects of CQD on general physiological indexes in rats

Based on the results of our network pharmacology analysis, we then evaluated the therapeutic effect of CQD in a rat model of HUA. After drug intervention, the urine volume of the Model group was significantly decreased compared with that of the Control group ($P < 0.01$), while the volume was significantly increased in the CQD group ($P < 0.05$); however, there was no significant change in urine volume in the Allo group (Fig. 4a). These findings suggested that CQD treatment significantly increases urine output, which promotes UA excretion, while Allo group did not. The kidney index of rats in the Model group was significantly higher than that in the Control group ($P < 0.01$), while that of the CQD group was significantly lower. The kidney index of rats in the Allo group did not decrease significantly, but increased significantly compared with that of the Control group ($P < 0.01$) (Fig. 4b). In terms of gross appearance, the kidneys in the Control group were ruddy in color and normal in shape. (Supplement Figure S2), while those in the Model group showed marked swelling and pallor, with white particles on the surface that were suspected to be urate particles. The kidneys in the CQD group appeared relatively normal, without obvious lesions, while those in the Allo group showed obvious swelling and pallor, but no white particles were observed on the surface.

3.3.2. Effects of CQD on biochemical indexes in rats

After day 3 of intervention, the SUA in the Model group was significantly higher than that in the Control group ($P < 0.05$), and a further increase of SUA was observed obvious after day 7 ($P < 0.01$). Compared with the Model group at day 3, the SUA concentrations of the CQD and Allo groups were decreased slightly, with significant differences between the treatment and Model groups apparent at day 7 ($P < 0.05$ and $P < 0.01$, respectively). Furthermore, the decrease in SUA concentrations was more marked in the Allo group than that in the CQD group (Fig. 4c). In addition, the UUA level in the Model group was increased compared with that in the Control group, while it was decreased after treatment, although the effect was but not statistically significant (Fig. 4d). Similar alterations were observed in the levels of SCr and BUN (Fig. 4e and f). Compared with the Control group, increased levels of SCr and BUN were observed in the Model group on day 3 of the intervention, although only the change in BUN was statistically significant ($P < 0.01$). Furthermore, compared with the Model group, the levels of SCr and BUN decreased in the CQD group, although the change was not statistically significant. Furthermore, while the levels of SCr and BUN in the Allo group did not change significantly compared with those in the Model group, the levels were significantly increased compared with Control group ($P < 0.05$). On day 7 of the intervention, the changes observed were more marked, with significant increases in the levels of SCr and BUN in the Model group compared to those in the Control group ($P < 0.05$ and $P < 0.01$, respectively). The levels of SCr and BUN in the CQD group were significantly lower than those in the Model group ($P < 0.05$ and $P < 0.01$, respectively). While the levels of SCr and BUN in the Allo group did not change significantly compared with those in the Model group, the levels were significantly increased compared with those in the Control group ($P < 0.01$). These results showed that the levels of SUA, SCr and BUN in the Model group increased significantly over time compared with those in the Control group. Both CQD and Allo treatment reduced SUA levels. CQD treatment alleviated kidney injury, while Allo treatment did not.

3.3.3. Effects of CQD on kidney histopathology in rats

Histopathological results showed that there were no obvious pathological changes in the Control group; the shape of the glomerulus and renal tubules were normal, and there were no abnormalities in the renal interstitium, although a few inflammatory cells were observed. Marked pathological changes were observed in the kidneys of the Model group; large areas of blood stasis, obvious tubular dilation and epithelial cell shedding, were observed with severe inflammatory cell infiltration, and occasional eosinophilic degeneration and cell necrosis. The trend of renal tubular dilation in the CQD group was less marked than that in the Model group, and the glomerular morphology was relatively intact, with occasional mild inflammatory cell infiltration. However, the degree of renal tubular dilatation in the Allo group was greater than that in the Model group, with infiltration by numerous inflammatory cells (Fig. 4g). Gomori staining revealed that there was no urate crystal deposition in the Control group, while the deposition was marked in the Model group. However, only few urate crystals were observed locally in the CQD and Allo groups (Fig. 4h).

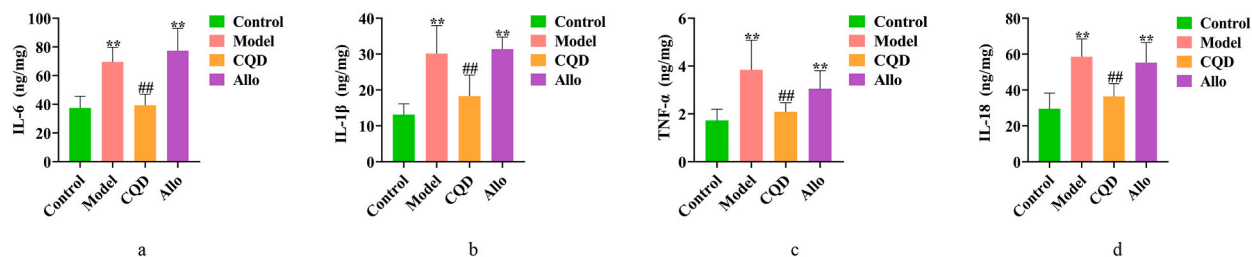


Fig. 5. ELISA analysis of the effects of CQD on the relative content of (a) IL-6, (b) TNF- α , (c) IL-1 β , (d) IL-18. Data represent the mean \pm SD ($n = 6$). * $P < 0.05$ and ** $P < 0.01$ vs. Control group. # $P < 0.05$ and ## $P < 0.01$ vs. Model group.

3.4. Effect of CQD on inflammatory factors levels in rat serum

Compared with the Control group, serum levels of inflammatory factors (IL-6, TNF- α , IL-1 β and IL-18) were significantly increased in the Model group ($P < 0.01$). Compared with the Model group, the serum levels of all inflammatory factors in the CQD group were significantly decreased ($P < 0.01$), while the levels in the Allo group were significantly increased, with slightly higher levels of IL-6 and IL-1 β in the Allo group than those in the Model group (Fig. 5a–d).

3.5. Effect of CQD on mRNA expression of ABCG2, NLRP3 and caspase3

Compared with the Control group, mRNA expression of ABCG2 in the Model group was significantly downregulated ($P < 0.01$), while after CQD and Allo treatment, its expression was significantly upregulated ($P < 0.01$) (Fig. 6a). In contrast, mRNA expression of NLRP3 and caspase3 was significantly upregulated compared with that in the Control group ($P < 0.01$ and $P < 0.05$, respectively) (Fig. 6b and c), while the levels were significantly downregulated after CQD treatment ($P < 0.01$ and $P < 0.05$, respectively). There was no significant difference in mRNA expression of caspase3 in the Allo group compared with that in the Control group, while the mRNA expression of NLRP3 was significantly upregulated ($P < 0.01$).

3.6. Effect of CQD on ABCG2 and NLRP3 protein expression

As shown in Fig. 6d, the expression of ABCG2 protein in the Model group was significantly decreased compared with the Control group, while its expression significantly increased in the CQD and Allo groups ($P < 0.05$ and $P < 0.01$, respectively) (Fig. 6e). The opposite pattern of changes was observed for NLRP3 protein expression. Compared with the Control group, NLRP3 protein expression in the Model and Allo groups was significantly increased ($P < 0.01$), while that in the CQD group was significantly lower than that in the Model group ($P < 0.01$) (Fig. 6f). The original images without adjustment are shown in the supplementary file figure s3. These findings suggested that CQD and Allo groups reduce UA by increasing ABCG2 expression at both the mRNA and protein levels, although only CQD provided renal protection by downregulating the mRNA and protein expression of NLRP3 expression at both the mRNA and protein levels and reducing the levels of inflammatory factors.

4. Discussion

According to modern medicine, HUA is a chronic metabolic disease caused by dysregulation of purine metabolism. According to TCM, the pathogenesis of HUA is complex and caused mainly by insufficient endowment, exogenous pathogenic factors, seven emotions and internal injuries, improper diet, deficiency of viscera, dampness, phlegm, and blood stasis, with the main disease location in the spleen and kidney [34]. Most of the commonly used clinical drugs are single drug components with direct effects on a single target. However, the multi-component, multi-target characteristics of TCM are more conducive to improving various symptoms of

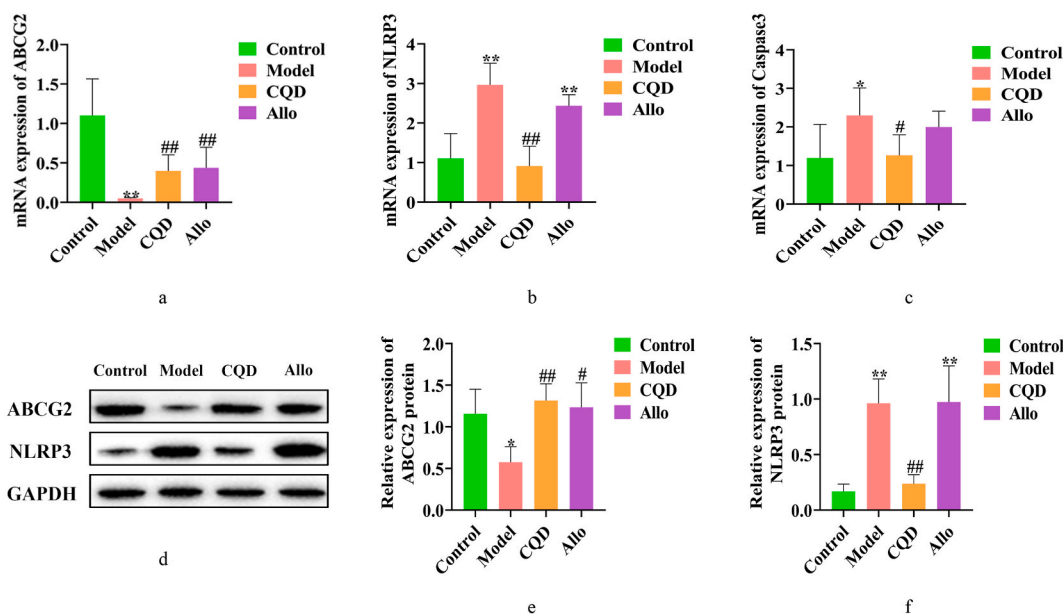


Fig. 6. Analysis of the effect of CQD on mRNA expression of (a) ABCG2, (b) NLRP3, (c) caspase3. Effect of CQD on the protein expression of (d) ABCG2 and NLRP3. Data represent the mean \pm SD (PCR: $n = 6$; Western blot: $n = 3$). * $P < 0.05$ and ** $P < 0.01$ vs. Control group. # $P < 0.05$ and ## $P < 0.01$ vs. Model group.

HUA, thereby providing a more comprehensive treatment approach.

All four herbs in CQD have been included in the 2020 edition of the Chinese Pharmacopoeia [35]. According to the Pharmacopoeia, we selected genipinic acid and verbascoside to verify cheqianzi, typhaneoside and isorhamnetin-3-O-neohesperidoside to verify puhuang and β -ecdysterone as the critical marker of the quality of niuxi. However, there is no corresponding quality standard for sangbaipi, chlorogenic acid has been widely used for this purpose [28,36]. In validate chlorogenic acid as a specific marker to assess the quality of sangbaipi in CQD, we detected its presence in each herb and confirmed that the other three herbs did not contain chlorogenic acid.

The emergence of network pharmacology has provided a solution to studying complex TCMS, with their multiple components, targets and interactions. This discipline has facilitated transformation of the “single target, single drug” model to the “network target, multi-component therapy” model that can be used to predict and screen the effective components and related targets of TCMS, as well as their potential mechanisms of action [37]. Previous network pharmacology analysis of the mechanism underlying the therapeutic effects of Plantaginis Herba in HUA has provided promising new treatment strategies [15]. To obtain the most comprehensive effective chemical components of CQD, we study searched the literature published in recent years on the detection of TCM components in each herb. The BATMAN-TCM database was used to integrate the targets of each of the identified components according to the score to obtain a set of related targets of CQD. A set of 99 core HUA-related targets were used to construct the CQD-compound-target-disease interaction network. The network was found to contain the UA-related transporter ABCG2, suggesting that CQD may mediate a reduction in UA, which is consistent with the efficacy reported in ancient texts. IL-6, TNF- α , IL-1 β , IL-18, caspase3 and NLRP3 were also included in the network, and the scores of these inflammatory factors were generally high. These targets indicate that CQD also regulates inflammation and apoptosis, suggesting that CQD has nephroprotective effects [38]. The GO and KEGG functional enrichment analysis showed that the role of CQD was related to the regulation of defense response and lipid and atherosclerosis pathways, suggesting key roles for the pathways in the therapeutic effects of CQD on HUA, although further research is required to fully elucidate the underlying mechanism.

Subsequently, we conducted in vivo pharmacodynamic studies in animals to verify the network pharmacology predictions of targets associated with the therapeutic effect of CQD on HUA. Compared with the Model group, CQD promoted urination, significantly decreased the level of SUA, and reduced the black crystals of urate in the kidney, indicating that CQD mediates a reduction in UA. CQD has shown excellent UA-lowering effects in animal models. HUA is often accompanied by kidney injury, which can lead to vascular and tubulointerstitial lesions that accelerate the progression of chronic kidney disease [3]. UA activates the immune system and changes the characteristics of resident renal cells, such as tubular epithelial cells, endothelial cells, and vascular smooth muscle cells to a proinflammatory and profibrotic state [39]. Therefore, effective treatment of HUA with kidney injury requires drugs with the capacity to both reduce UA levels and provide renal protection; however, while the drugs commonly used in clinical practice generally have good UA-lowering effects, the renal protection is less effective. In our study, we found that Allo significantly reduced UA levels compared with those in the Control group, but without obvious renal protection, and even tended to exacerbate kidney injury over time. Most of the drugs currently used to treat HUA in clinical practice have the same disadvantages as Allo, which is widely used [40]. We showed that CQD significantly reduced the renal index and levels of SCr and BUN. Furthermore, HE staining indicated that the degree of kidney injury in the CQD group was significantly reduced compared with the Model group, confirming that CQD has a better therapeutic effect on HUA with kidney injury.

We also performed network pharmacology analysis to clarify the mechanism underlying the therapeutic effects of CQD on HUA. ABCG2 was originally discovered in multidrug-resistant breast cancer cell lines [32]. Urate homeostasis in humans is a complex process involving urate biosynthesis, renal urate reabsorption, and renal and intestinal urate excretion. Dysregulated UA excretion is one of the common causes of HUA, and ABCG2 is involved in the elimination of urate [41]. Thus, ABCG2 is implicated as a therapeutic target for HUA. In a recent study, a new antidiabetic agent was shown to promote the expression of the UA transporter ABCG2, p-AMPK, p-AKT and p-CREB proteins in the kidney and ileum. The same trend was observed in human tubular epithelial (HK-2) cells in vitro. These changes indicate that ABCG2 is indeed closely related to the reduction of UA [42]. When evaluating the effect of Yi-Suan-Cha and exploring its mechanism of action, it was found that the increased expression of ABCG2 in the kidney did indeed increase the UA excretion, and cooperated with various transporters in vivo to reduce UA [43]. In addition, a retrospective cohort study showed that dysfunction in ABCG2 can lead to elevated serum UA concentrations, with persistent high UA increasing the risk of induced renal injury. Furthermore, the conditions are more severe in individuals with highly dysfunctional ABCG2 [44]. This new finding highlights the potential importance of ABCG2 in the pathogenesis of HUA-induced kidney injury. In our study, using a rat model of HUA, we found that the SUA level was significantly increased in the Model group, and ABCG2 expression was significantly reduced at both the mRNA and protein levels. In contrast, the levels of SUA were significantly decreased after CQD and Allo administration, and ABCG2 expression was significantly increased in both groups. The beneficial effects on UA excretion indicate that CQD reduces UA by upregulating ABCG2 expression to promote UA excretion, thereby alleviating kidney injury.

In addition, the inflammatory factors IL-6, TNF- α , IL-1 β , IL-18, and NLRP3 were also identified as core targets in the network. NLRP3, is a member of a cytoplasmic protein complex that can recognize various stresses, exogenous microorganisms, and endogenous danger signals, activates caspase-1 and induces the production of IL-1 β and IL-18 [45]. In recent years, accumulating evidence has demonstrated that HUA-induced autophagy and NLRP3-dependent inflammation are closely related to the development of kidney injury [46,47], and the inflammatory response leads to apoptosis. In addition, caspase3, an apoptosis-related target in the network, was also assigned a high score as a CQD target. NLRP3 inflammasome activation has been shown to mediate diverse chronic kidney diseases through regulation of proinflammatory cytokines, tubulointerstitial injury, glomerular diseases, renal inflammation, and fibrosis pathways. Autophagy is a characterized by negative regulation of the NLRP3 inflammasome, and some drugs can achieve renoprotective effects through the inhibition of NLRP3 inflammasome activation by inducing autophagy [48]. Recent studies have

shown that UA upregulates autophagy and further activates the NLRP3 inflammasome, leading to pyroptotic cell death. In vitro and in vivo studies showed that blockade of autophagy improves UA-induced pyroptosis by inhibiting autophagic-inflammasome pathways, preventing the occurrence of hyperuricemic nephropathy [49]. In addition, following NLRP3 inflammasome and cytokine abundance were found to be significantly increased in macrophages treated with UA, while miR-223 provided negative feedback regulation of inflammatory development by inhibiting the production of IL-1 β and TNF- α . Thus, these findings provided evidence that UA regulates cytokine production by targeting the NLRP3 inflammasome [50]. In this study, NLRP3 inflammasome expression was significantly downregulated at the mRNA and protein levels in the CQD group compared with the Model group, suggesting that CQD exerts a nephroprotective effect by inhibiting NLRP3 expression and thus, reducing cytokine levels.

In summary, our network and experimental pharmacology analyses demonstrated that CQD significantly reduced UA, inhibited inflammatory responses, reduced apoptosis, and protected kidneys, thus providing new evidence to support the application of CQD in the treatment of HUA with kidney injury. However, the related pathways of network pharmacology still need to be verified by further studies, so as to further investigate the mechanism of action of CQD on HUA treatment and lay the foundation for clinical drug development.

5. Conclusion

In this study, it is found that CQD reduces UA by acting on the ABCG2 transporter, while inhibiting the NLRP3 inflammasome to improve inflammatory responses, and reduce apoptosis, thereby exerting a protective effect on the kidneys. These results implicate CQD as a promising TCM candidate for the treatment of HUA with kidney injury.

Author contribution statement

Jing Meng: Conceived and designed the experiments; Performed the experiments; Analyzed and interpreted the data; Wrote the paper.

Jingzhuo Tian: Conceived and designed the experiments; Analyzed and interpreted the data.

Yong Zhao; Suyan Liu; Chenyue Liu; Chunying Li: Contributed reagents, materials, analysis tools or data.

Yan Yi; Yushi Zhang; Jiayin Han; Lianmei Wang; Chen Pan; Fang Wang; Xuan Tang; Dunfang Wang; Shasha Qin: Performed the experiments.

Aihua Liang: Conceived and designed the experiments; Contributed reagents, materials, analysis tools or data.

Funding statement

This study was financially supported by National Natural Science Foundation of China (No.82192913, 82174073), Qihuang Scholar Program and China Academy of Chinese Medical Sciences (CI2021B016, CI2021A04801, CI2021A04803, ZXKT20022).

Data availability statement

Data will be made available on request.

Declaration of interest's statement

The authors declare that they have no known competing financial interests or personal relationships that could have appeared to influence the work reported in this paper.

Abbreviations

CQD	Cheqianzi Decoction
TCM	Traditional Chinese Medicine
UA	uric acid
HUA	hyperuricemia
HPLC	high performance liquid chromatography
SUA	serum uric acid
SCr	serum creatinine
BUN	blood urea nitrogen
ABCG2	adenosine triphosphate (ATP)-binding cassette efflux transporter G2
NLRP3	NOD-like receptor family member 3
Ethb	ethambutol
AD	adenine
Allo	allopurinol
HE	hematoxylin eosin
IL-6	interleukin-6

TNF- α	tumor necrosis factor- α
IL-1 β	interleukin-1 β
IL-18	interleukin-18
ELISA	enzyme-linked immunosorbent assay
CNKI	China National Knowledge Infrastructure
GO	Gene ontology
KEGG	Kyoto Encyclopedia of Genes and Genomes

Appendix A. Supplementary data

Supplementary data to this article can be found online at <https://doi.org/10.1016/j.heliyon.2023.e15333>.

References

- [1] M. Zhang, X. Zhu, J. Wu, Z. Huang, Z. Zhao, X. Zhang, Y. Xue, W. Wan, C. Li, W. Zhang, L. Wang, M. Zhou, H. Zou, L. Wang, Prevalence of hyperuricemia among Chinese adults: findings from two nationally representative cross-sectional surveys in 2015-16 and 2018-19, *Front. Immunol.* 12 (2022), 791983, <https://doi.org/10.3389/fimmu.2021.791983>.
- [2] C. Borghi, E. Agabiti-Rosei, R.J. Johnson, J.T. Kielstein, E. Lurbe, G. Mancia, J. Redon, A.G. Stack, K.P. Tsoufis, Hyperuricaemia and gout in cardiovascular, metabolic and kidney disease, *Eur. J. Intern. Med.* 80 (2020) 1–11, <https://doi.org/10.1016/j.ejim.2020.07.006>.
- [3] C. Ponticelli, M.A. Podestà, G. Moroni, Hyperuricemia as a trigger of immune response in hypertension and chronic kidney disease, *Kidney Int.* 98 (2020) 1149–1159, <https://doi.org/10.1016/j.kint.2020.05.056>.
- [4] X. Feng, J. Huang, Y. Peng, Y. Xu, Association between decreased thyroid stimulating hormone and hyperuricemia in type 2 diabetic patients with early-stage diabetic kidney disease, *BMC Endocr. Disord.* 21 (2021) 1, <https://doi.org/10.1186/s12902-020-00672-8>.
- [5] W. Feng, D. Cui, T. Yang, Key point interpretation of Chinese guidelines for diagnosis and treatment of hyperuricemia and gout (2019), *Chin. J. Intern. Med.* 37 (2020) 528–531, <https://doi.org/10.3969/j.issn.1001-9057.2020.07.022>.
- [6] X. Xu, J. Hu, N. Song, R. Chen, T. Zhang, X. Ding, Hyperuricemia increases the risk of acute kidney injury: a systematic review and meta-analysis, *BMC Nephrol.* 18 (2017) 27, <https://doi.org/10.1186/s12882-016-0433-1>.
- [7] C. Jennings, I. Mackenzie, T. MacDonald, Review of hyperuricaemia and hypertension: a target for treatment, *J. Hypertens.* 3 (2014), 1000164, <https://doi.org/10.4172/2167-1095.1000164>.
- [8] R.C. Heel, R.N. Brogden, T.M. Speight, G.S. Avery, Benzbromarone: a review of its pharmacological properties and therapeutic use in gout and hyperuricaemia, *Drugs* 14 (1977) 349–366, <https://doi.org/10.2165/00003495-197714050-00002>.
- [9] S.V. Badve, E.M. Pascoe, A. Tikou, N. Boudville, F.G. Brown, A. Cass, P. Clarke, N. Dalbeth, R.O. Day, J.R. de Zoysa, B. Douglas, R. Faull, D.C. Harris, C. M. Hawley, G. Jones, J. Kanellis, S.C. Palmer, V. Perkovic, G.K. Rangan, D. Reidlinger, L. Robison, R.J. Walker, G. Walters, D.W. Johnson, Effects of allopurinol on the progression of chronic kidney disease, *N. Engl. J. Med.* 382 (2020) 2504–2513, <https://doi.org/10.1056/NEJMoa1915833>.
- [10] H. Yuan, J. Li, Y. Feng, Literature analysis on 114 cases of allopurinol-induced adverse drug reactions, *Chin. J. Drug Appl. Monit.* 13 (2016) 359–362.
- [11] Adverse drug reaction monitoring center, Adverse drug reaction information bulletin – be alert to the risk of liver damage induced by benzbromarone, *Chin. J. PV* 13 (2016) 59–60, <https://doi.org/10.19803/j.1672-8629.2016.01.018>.
- [12] W.B. White, K.G. Saag, M.A. Becker, J.S. Borer, P.B. Gorelick, A. Whelton, B. Hunt, M. Castillo, L. Gunawardhana, Cardiovascular safety of febuxostat or allopurinol in patients with gout, *N. Engl. J. Med.* 378 (2018) 1200–1210, <https://doi.org/10.1056/NEJMoa1710895>.
- [13] Z. Wei, J. Zhang, H. Li, J. Wu, Y. Liu, B. Gu, Overview on the mechanism of single traditional Chinese medicine in reducing uric acid, *Tradit. Chin. Med. J* 20 (2021) 69–72, <https://doi.org/10.14046/j.cnki.zyytb2002.2021.06.020>.
- [14] C. Zhu, B. Zhang, Z. Lin, H. Niu, X. Wang, H. Wang, L. Li, Research progress of traditional Chinese medicine in the treatment of hyperuricemia, *Chin. J. Tradit. Chin. Med. Pharm* 30 (2015) 4374–4376.
- [15] R. Tang, X. Peng, Y. Wang, X. Zhou, H. Liu, Network pharmacology-Based, Investigation of the mechanism of action of Plantaginis Herba in hyperuricemia treatment, *Evid. Based Complement. Alternat. Med.* 2021 (2021), 5595384, <https://doi.org/10.1155/2021/5595384>.
- [16] F. Yang, W. Shi, L. Wang, N. Qin, C. Wang, Y. Guo, G. Xu, J. Fang, X. Yu, Q. Ma, Lipidomics study of the therapeutic mechanism of Plantaginis Semen in potassium oxonate-induced hyperuricemia rat, *BMC Complement. Med. Ther.* 21 (2021) 175, <https://doi.org/10.1186/s12906-021-03350-x>.
- [17] J. Zeng, B. Xu, J. Wang, Y. Bi, X. Wang, G. Zhong, G. Ren, J. Zhu, M. Li, Y. Zhu, Hypouricemic effects of acteoside and isoacteoside from Plantaginis Semen on mice with acute hyperuricemia and their possible mechanisms, *Chin. Tradit. Pat. Med.* 38 (2016) 1449–1454, <https://doi.org/10.3969/j.issn.1001-1528.2016.07.003>.
- [18] S. Wang, M. Zeng, B. Li, Y. Kan, B. Zhang, X. Zheng, W. Feng, Raw and salt-processed *Achyranthes bidentata* attenuate LPS-induced acute kidney injury by inhibiting ROS and apoptosis via an estrogen-like pathway, *Biomed. Pharmacother.* 129 (2020), 110403, <https://doi.org/10.1016/j.biopha.2020.110403>.
- [19] Y. Dang, D. Liang, X. Zhou, Y. Qin, Y. Gao, W. Li, Protective effect of Mori Cortex on kidney in rats with hyperlipidemia and hyperuricemia based on molecular docking technique, *Chin. Tradit. Herb. Drugs* 50 (2019) 1175–1181, <https://doi.org/10.7501/j.issn.0253-2670.2019.05.022>.
- [20] K. Gao, Y. Zhu, H. Wang, X. Gong, Z. Yue, A. Lv, X. Zhou, Network pharmacology reveals the potential mechanism of Baiying Qinghou decoction in treating laryngeal squamous cell carcinoma, *Ageing* 13 (2021) 26003–26021, <https://doi.org/10.18632/ageing.203786>.
- [21] Y. Tang, C. Shi, Y. Qin, S. Wang, H. Pan, M. Chen, X. Yu, Y. Lou, G. Fan, Network pharmacology-based investigation and experimental exploration of the antiapoptotic mechanism of colchicine on myocardial ischemia reperfusion injury, *Front. Pharmacol.* 12 (2021), 804030, <https://doi.org/10.3389/fphar.2021.804030>.
- [22] W. Ni, P. Cheng, Study on herbal dosage in the Song and Yuan dynasties, *Acta Univ. Tradit. Med. Sin. Pharmacol. Shanghai* 28 (2014) 23–25+42, <https://doi.org/10.16306/j.1008-861x.2014.01.023>.
- [23] Z. Liu, F. Guo, Y. Wang, C. Li, X. Zhang, H. Li, L. Diao, J. Gu, W. Wang, D. Li, F. He, BATMAN-TCM: a bioinformatics analysis tool for molecular mechanism of traditional Chinese medicine, *Sci. Rep.* 6 (2016), 21146, <https://doi.org/10.1038/srep21146>.
- [24] L. Perlman, A. Gottlieb, N. Atias, E. Ruppin, R. Sharan, Combining drug and gene similarity measures for drug-target elucidation, *J. Comput. Biol.* 18 (2011) 133–145, <https://doi.org/10.1089/cmb.2010.0213>.
- [25] D. Szklarczyk, A.L. Gable, K.C. Nastou, D. Lyon, R. Kirsch, S. Pyysalo, N.T. Doncheva, M. Legeay, T. Fang, P. Bork, L.J. Jensen, C. von Mering, The STRING database in 2021: customizable protein-protein networks, and functional characterization of user-uploaded gene/measurement sets, *Nucleic Acids Res.* 49 (2021) D605–D612, <https://doi.org/10.1093/nar/gkaa1074>.
- [26] J. Meng, J. Tian, L. Wang, Y. Zhao, C. Li, Y. Yi, Y. Zhang, J. Han, C. Pan, S. Liu, Z. Xian, D. Wang, S. Qin, F. Wang, A. Liang, Adequate animal models of hyperuricemia for traditional Chinese medicine screening, *Chin. J. Exp. Tradit. Med. Formulae* 27 (2021) 46–56, <https://doi.org/10.13422/j.cnki.syfx.20211601>.

- [27] T. Yuan, T. Zheng, L. Xie, S. Cheng, Y. Wei, Z. Ouyang, Simultaneous determination of five constituents in *Morus alba* by HPLC, *Chin. Tradit. Pat. Med.* 41 (2019) 1606–1611, <https://doi.org/10.3969/j.issn.1001-1528.2019.07.024>.
- [28] H. Yan, H. Gao, Q. Cui, R. Rong, Q. Lv, Simultaneous determination of four ingredients in *Mori Cortex* by HPLC, *Chin. J. Exp. Tradit. Med. Formulae* 23 (2017) 53–56, <https://doi.org/10.13422/j.cnki.Syfx.2017050053>.
- [29] H. Xian, Y. Liu, A. Rundberg Nilsson, R. Gatchalian, T.R. Crother, W.G. Tourtellotte, Y. Zhang, G.R. Aleman-Muench, G. Lewis, W. Chen, S. Kang, M. Luevanos, D. Trudler, S.A. Lipton, P. Soroosh, J. Teijaro, J.C. de la Torre, M. Ardit, M. Karin, E. Sanchez-Lopez, Metformin inhibition of mitochondrial ATP and DNA synthesis abrogates NLRP3 inflammasome activation and pulmonary inflammation, *Immunity* 54 (2021) 1463–1477, <https://doi.org/10.1016/j.immuni.2021.05.004>.
- [30] J. Xiao, X.L. Zhang, C. Fu, R. Han, W. Chen, Y. Lu, Z. Ye, Soluble uric acid increases NALP3 inflammasome and interleukin-1 β expression in human primary renal proximal tubule epithelial cells through the Toll-like receptor 4-mediated pathway, *Int. J. Mol. Med.* 35 (2015) 1347–1354, <https://doi.org/10.3892/ijmm.2015.2148>.
- [31] H.L. Hutton, J.D. Ooi, S.R. Holdsworth, A.R. Kitching, The NLRP3 inflammasome in kidney disease and autoimmunity, *Nephrology* 21 (2016) 736–744, <https://doi.org/10.1111/nep.12785>.
- [32] S. Kukal, D. Guin, C. Rawat, S. Bora, M.K. Mishra, P. Sharma, P.R. Paul, N. Kanojia, G.K. Grewal, S. Kukreti, L. Saso, R. Kukreti, Multidrug efflux transporter ABCG2: expression and regulation, *Cell. Mol. Life Sci.* 78 (2021) 6887–6939, <https://doi.org/10.1007/s00018-021-03901-y>.
- [33] K. Ichida, H. Matsuo, T. Takada, A. Nakayama, K. Murakami, T. Shimizu, Y. Yamanashi, H. Kasuga, H. Nakashima, T. Nakamura, Y. Takada, Y. Kawamura, H. Inoue, C. Okada, Y. Utsumi, Y. Ikebuchi, K. Ito, M. Nakamura, Y. Shinohara, M. Hosoyamada, Y. Sakurai, N. Shinomiya, T. Hosoya, H. Suzuki, Decreased extra-renal urate excretion is a common cause of hyperuricemia, *Nat. Commun.* 3 (2012) 764, <https://doi.org/10.1038/ncomms1756>.
- [34] W. Ye, Y. Cheng, X. Qiu, Research progress in the treatment of hyperuricemia with traditional Chinese medicine, *Hainan Med. J.* 31 (2020) 1187–1190, <https://doi.org/10.3969/j.issn.1003-6350.2020.09.029>.
- [35] Chinese Pharmacopoeia Commission, *Chinese Pharmacopoeia*, China Medical Science Press, Beijing, 2020, 70, 74, 311, 368–369.
- [36] Z. Chen, M. Meng, Y. Yang, X. Du, Z. Yang, H. Ren, Content determination of 6 active components in *Morus alba* by HPLC, *China Pharm.* 29 (2018) 911–914, <https://doi.org/10.6039/j.issn.1001-0408.2018.07.11>.
- [37] R. Zhang, X. Zhu, H. Bai, K. Ning, Network pharmacology databases for traditional Chinese medicine: review and assessment, *Front. Pharmacol.* 10 (2019) 123, <https://doi.org/10.3389/fphar.2019.00123>.
- [38] H.Y. Su, C. Yang, D. Liang, H.F. Liu, Research advances in the mechanisms of hyperuricemia-induced renal injury, *BioMed Res. Int.* 2020 (2020), 5817348, <https://doi.org/10.1155/2020/5817348>.
- [39] S.W. Jung, S.M. Kim, Y.G. Kim, S.H. Lee, J.Y. Moon, Uric acid and inflammation in kidney disease, *Am. J. Physiol. Ren. Physiol.* 318 (2020) F1327–F1340, <https://doi.org/10.1152/ajprenal.00272.2019>.
- [40] A. Rey, B. Batteux, S.M. Laville, J. Marienne, K. Masmoudi, V. Gras-Champel, S. Liabeuf, Acute kidney injury associated with febuxostat and allopurinol: a post-marketing study, *Arthritis Res. Ther.* 21 (2019) 229, <https://doi.org/10.1186/s13075-019-2011-y>.
- [41] R. Eckenstaler, R.A. Benndorf, The role of ABCG2 in the pathogenesis of primary hyperuricemia and gout—an update, *Int. J. Mol. Sci.* 22 (2021) 6678, <https://doi.org/10.3390/ijms22136678>.
- [42] Y. Lu, Y. Chang, T. Li, F. Han, C. Li, X. Li, M. Xue, Y. Cheng, Z. Meng, Z. Han, B. Sun, L. Chen, Empagliflozin attenuates hyperuricemia by upregulation of ABCG2 via AMPK/AKT/CREB signaling pathway in type 2 diabetic mice, *Int. J. Biol. Sci.* 16 (2020) 529–542, <https://doi.org/10.7150/ijbs.33007>.
- [43] Y. Qin, X. Zhang, H. Tao, Y. Wu, J. Yan, L. Liao, J. Meng, F. Lin, Ameliorative effect and mechanism of Yi-Suan-Cha against hyperuricemia in rats, *J. Clin. Lab. Anal.* 35 (2021), e23859, <https://doi.org/10.1002/jcla.23859>.
- [44] Y. Ohashi, S. Kuriyama, T. Nakano, M. Sekine, Y. Toyoda, A. Nakayama, T. Takada, Y. Kawamura, T. Nakamura, H. Matsuo, T. Yokoo, K. Ichida, Urate transporter ABCG2 function and asymptomatic hyperuricemia: a retrospective cohort study of CKD progression, S0272-6386, 00769-7. Advance online publication, *Am. J. Kidney Dis.* (2022), <https://doi.org/10.1053/j.ajkd.2022.05.010>.
- [45] Y. Zhen, H. Zhang, NLRP3 inflammasome and inflammatory bowel disease, *Front. Immunol.* 10 (2019) 276, <https://doi.org/10.3389/fimmu.2019.00276>.
- [46] M. Wu, Y. Ma, X. Chen, N. Liang, S. Qu, H. Chen, Hyperuricemia causes kidney damage by promoting autophagy and NLRP3-mediated inflammation in rats with urate oxidase deficiency, *Dis. Model. Mech.* 14 (2021), dmm048041, <https://doi.org/10.1242/dmm.048041>.
- [47] R.T. Keenan, The biology of urate, *Semin. Arthritis Rheum.* 50 (2020) S2–S10, <https://doi.org/10.1016/j.semarthrit.2020.04.007>.
- [48] Y. Wang, Y. Chen, C. Hsiao, M. Pan, B. Wang, Y. Chen, C. Ho, K. Huang, R. Chen, Induction of autophagy by pterostilbene contributes to the prevention of renal fibrosis via attenuating NLRP3 inflammasome activation and epithelial-mesenchymal transition, *Front. Cell Dev. Biol.* 8 (2020) 436, <https://doi.org/10.3389/fcell.2020.00436>.
- [49] Y. Hu, Y. Shi, H. Chen, M. Tao, X. Zhou, J. Li, X. Ma, Y. Wang, N. Liu, Blockade of autophagy prevents the progression of hyperuricemic nephropathy through inhibiting NLRP3 inflammasome-mediated pyroptosis, *Front. Immunol.* 13 (2022), 858494, <https://doi.org/10.3389/fimmu.2022.858494>.
- [50] Q. Zhang, D. Zhu, F. Dai, Y. Huang, J. Zheng, Y. Tang, Z. Dong, X. Liao, Y. Qing, MicroRNA-223 suppresses IL-1 β and TNF- α production in gouty inflammation by targeting the NLRP3 inflammasome, *Front. Pharmacol.* 12 (2021), 637415, <https://doi.org/10.3389/fphar.2021.637415>.